Korean J. Chem. Eng., 33(8), 2319-2324 (2016)
DOI: 10.1007/s11814-016-0089-3

pISSN: 0256-1115
eISSN: 1975-7220

A selective catalyst for methanol conversion into light olefin with a high propylene to ethylene ratio

Hamed Rashidi*, Ahmad Shariati*, Mohammad Reza Khosravi-Nikou*,†, and Touba Hamoule**

*Gas Engineering Department, Petroleum University of Technology, Ahwaz, Iran
**Science Department, Petroleum University of Technology, Ahwaz, Iran

(*Received 7 December 2015 • accepted 31 March 2016*)

Abstract−MSU-S catalyst, assembled from ZSM-5 zeolite seed (MFI), was synthesized with silica to alumina ratio 55 and characterized by XRD, NH3-TPD, BET and FT-IR techniques. It was tested in a vertical fixed bed reactor for selective production of light olefins from methanol (MTO) at temperatures of 400, 450 and 500 °C and WHSV of 1, 5 and 25 h^{-1}. After thorough investigation, it was found that WHSV=5 h^{-1} and temperature of 500 °C are the optimum conditions for maximum light olefin yield, which was 52% with propylene to ethylene ratio of 4.57. Acidity of MSU-S was promoted by incorporation of phosphotungusticacid (HPW) and a direct method to reach high HPW dispersion and thermal stability. Maximum light olefin yield was observed over HPW-MSU-S at the optimum reaction conditions to be nearly 60% with propylene to ethylene ratio of 4.3.

Keywords: MSU-S Catalyst, Phosphotungusticacid, Mesoporous Catalyst, Methanol to Olefin

INTRODUCTION

Ethylene and propylene are large volume base petrochemicals [1]. Ethylene is a raw material for production of polyethylene, ethylene oxide, styrene, ethylene glycol and polyvinyl chloride. Propylene is the second largest petrochemical product throughout the world, and an important starting material for the production of polypropylene, propylene oxide and phenol, which has received much attention [2]. A growing demand for olefins and specially, propylene is anticipated for the future [3,4]. Production of olefins from methanol as an indirect production of light olefins (C_2-C_4) from natural gas has received much attention because of its economic advantages over conventional steam cracking of NGL, naphtha and other fractions of petroleum [3,5-8]. It can also provide a wider range of ethylene to propylene ratio, which is of more interest to meet market demands [1,4,9,10]. Olefins were first produced by the reaction of methanol over ZSM-5 (MFI) catalyst in the late 1970's by Mobil Corporation. This discovery was made when attempting to develop methanol to gasoline process (MTG) and named MTO. In MTG process, methanol is dehydrated to dimethyl ether (DME) and water, then based on a final reaction step this mixture is converted to higher olefins, aromatics and naphtenes [4,10,11]. ZSM-5 and silicoaluminaphosphate (SAPO-34) have received much attention in the MTO process [11]. SAPO-34 was first discovered in the 1980s at Union Carbide [4]. SAPO-34 is more attractive in the MTO process because of its narrow product distribution in the range of C_1-C_5 while over ZSM-5 products vary among the range of C_1-C_{10}. But SAPO-34 deactivates faster than ZSM-5 because large aromatics are not allowed to escape from its small pores [11]. Selectivity to light olefins is a challenge in MTO process, and there is constant research to develop novel catalysts for selective production of C_2-C_4 [3]. There is also a growing need to utilize technologies that favor higher ratios of propylene-to-ethylene production [2]. Previous works on Conventional catalysts have shown low $C_3^=/C_2^=$ production ratio (1 to 2.5 for ZSM-5; 0.14 to 1.66 for SAPO-34) [3,22,23]. Some works have been done to increase the $C_3^=/C_2^=$ production ratio by altering the process (up to 2.1 for SAPO-34) [4]. Therefore, there is a need to devise new processes or catalysts to increase the $C_3^=/C_2^=$ production ratio.

On the other hand, mesoporous catalysts have received much attention for their inherent high surface area and their applications in various processes either as active site or catalyst support. Pore dimensions of these catalysts can be tailored between 15 to 100 Å based on the usage. However, the inherent acidity of these materials is not as strong as zeolites [12]. Attempts have been made to improve the acidity strength of mesoporous chemicals recently, and a series of enhanced mesoporous materials like MSU-S (Michigan State University) [13] and MAS (highly ordered hexagonal mesoporous aluminosilicates) [14] have been prepared with direct incorporation of nano-clustered zeolite precursors [12].

In comparison to a conventional Al-MCM-41 sample, the MSU-S mesoporous aluminosilicates synthesized by incorporation of zeolite seeds exhibit high hydrothermal stability and increased acidity. With regard to acidity, the MSU-S materials were more active in some catalytic processes compared to Al-MCM-41 with similar Al content, indicating the higher acidity strength of the MSU-S materials. Therefore, MSU-S material can be considered as an effective acid solid catalyst for catalytic processes possessing high temperature [15].

In the present study, for the first time, MSU-S and HPW-MSU-S applicability in MTO reaction were investigated with a special focus on propylene to ethylene ratio.

[†] To whom correspondence should be addressed.

E-mail: mr.khosravi@put.ac.ir, khosravi_m@yahoo.com

EXPERIMENTAL

1. Catalyst Preparation

1-1. MSU-S Synthesis

Mesoporous MSU-S (MFI) catalyst was synthesized based on Liu et al. procedure [24]. Tetrapropylammonium hydroxide (10.2 g, Merck 40% aqueous solution), which is utilized for directing MFI structure, and deionized water (79.26 g) were mixed. Afterwards, Sodium aluminate (0.34 g, Aluminum source) and Cab-osil M5 (6 g, Silicon source) were added. Now, a milky solution was prepared, which was stirred for 18 h at 50 °C. The next step was to prepare a solution of deionized water (100 g) and hexadecyltrimethylammonium bromide (9.44 g, surfactant) and adding it to the milky solution.

The molar gel composition of the final solution would be $1SiO_2$: 0.018 Al_2O_3: 0.023 Na_2O: 0.266 HTABr: 0.2 TPAOH: 103.6 H_2O which was poured into a Teflon-lined stainless steel autoclave which was held at 150 °C for 48 h. After hydrothermal treatment, the product was filtered, washed and dried for 9 h at 85 °C. The dried sample was a white product which ion-exchanged with NH_4NO_3 (0.1 M in 96% ethanol) for 2 h at reflux temperature. The sample was dried at 95 °C for 12 h. The calcination of the sample was carried out at 550 °C in air for 10 h with heating rate of 1 °C/min.

1-2. HPW-MSU-S Synthesis

Phosphotungustic acid (HPW) doped MSU-S catalyst was synthesized based on the method proposed by Gagea et al. and named HPW-MSU-S. A direct synthesis (DS) method for the incorporation of HPW in the MSU-S structure was employed to attempt better dispersion of HPW. It is already known that HPW in impregnated samples undergoes decomposition at higher temperatures, and incorporation of HPW via DS method has shown high thermal stability [14].

Two solutions were prepared: (1) 10 wt% HPW (Phosphotungstic acid $H_3PW_{12}O_{40}$) and 100 g water were mixed and kept under stirring for 24 hours. Six hours later, (2) 10.2 g tetrapropylammonium hydroxide, 79.26 g of deionized water, 0.34 g of sodium aluminate and 6.0 g of Cab-osil M5 were mixed and kept under stirring at 50 °C for 18 hours. Then 9.44 g of Hexadecyltrimethylammonium bromide was mixed with solution (2). It was added to solution (1) and mixed thoroughly to produce gel. Then it was introduced to Teflon-lined stainless steel auto clave and kept under heating for 48 h at 150 °C. The rest of the preparation method was as the same as MSU-S synthesis described previously.

2. Characterization

Powder XRD patterns of obtained samples were carried out in 2θ range of 0-10° for MSU-S catalysts and 0-80° for pure Phosphotungstic acid and HPW-MSU-S catalyst by using an X-PERT Diffractometer equipped with Ni-filtered. N_2 adsorption of prepared samples was conducted at −196 °C by a NOVA 2200 instrument. To remove the moisture and any other possible adsorbates, it is preferred to run a degassing process (200 °C with N_2 flow for 16 h) prior to BET measurements.

A PulseChemiSorb 2705 instrument was used to determine the acidity of the catalysts via NH_3-TPD, which utilized a conventional flow apparatus and a TCD. Degassing was performed at 500 °C for 130 min with a helium flow rate of 55 ml/min. Afterwards, the sample was cooled to 100 °C and saturated with pure ammonia for 60 min. Then the sample was purged with a helium flow for 1 h to remove any NH_3 adsorbed on the surface of the sample. Next was cooling the sample to ambient temperature, then heating to 500 °C with a rate of 10 °C/min under helium flow rate of 30 ml/min. TCD measured the amount of ammonia in the effluent and recorded it as a function of temperature.

An 8400S Laboratories FT-IR spectrophotometer (Shimadzu, Japan) was used to determine the FT-IR spectra of samples; the instrument utilized was an MCT-NB cryogenic mercury detector (2 cm^{-1} resolution). Sample matrix and reference material was considered the potassium bromide (KBr); self-supporting discs pelleted powdered samples (25-30 mg cm^{-2} and 0.1-0.2 mm thick) were placed in the instrument and the IR test was performed at ambient temperature.

3. Activity Test

A vertical fixed bed micro reactor was used for catalytic conversion of methanol in the temperature range of 400 °C to 500 °C and 2 bara pressure, the length and internal diameter of the reactor was, respectively, 200 mm and 9 mm; a thermocouple was placed through the reactor bed to indicate the actual temperature of the catalyst bed in the reaction.

1.5 g of catalyst was used for each run of the reactor; quartz wool was placed at the top and the bottom of the catalyst bed. Prior to the activity test, catalyst was activated under flow of nitrogen at 500 °C for 2 h. Pure methanol was injected by means of an HPLC pump with an accuracy of 0.01 ml/min to a pre-heater conditioned at 250 °C prior to entering the reactor. Weight hourly space velocity (WHSV) was determined to be 1, 5 and 25 h^{-1} corresponding to liquid methanol flow rates of 0.03, 0.16 and 0.79 ml/min.

The reaction products were analyzed by an online GC (Young Lin 6000), a plot Q column (0.32 mm ID, 30 m length, 60 micron coating thickness) and an FID detector was employed. Reactor output line was heat-traced (200 °C) to avoid condensation of gaseous products. A constant flow of nitrogen (60 ml/min) was considered as carrier gas through the lines.

RESULTS AND DISCUSSION

1. Catalyst Characterization

1-1. XRD Results

Low and high angle XRD patterns of MSU-S catalyst are shown in Fig. 1(a)-(b). A distinct diffraction peak is illustrated in Fig. 1(a) which can be indexed to (1 0 0) diffraction line characteristic of hexagonal mesostructure [15]. Previous studies on supported heteropolyacids revealed the strong tendency to agglomeration of heteropoly acid molecules. A direct synthesis method for the incorporation of HPW into the MSU-S structure was conceived to attempt better dispersion of HPW. From Fig. 1(b), by looking at the high angle region XRD pattern of HPW-MSU-S, it was found that there was not any diffraction pattern of crystalline HPW phase. This is an evidence of the dispersed nature of HPW in HPW-MSU-S structure [13].

1-2. N_2 Adsorption-desorption Results

The N_2 adsorption-desorption isotherms for MSU-S and HPW-MSU-S catalysts are shown in Fig. 2. Both samples demonstrated

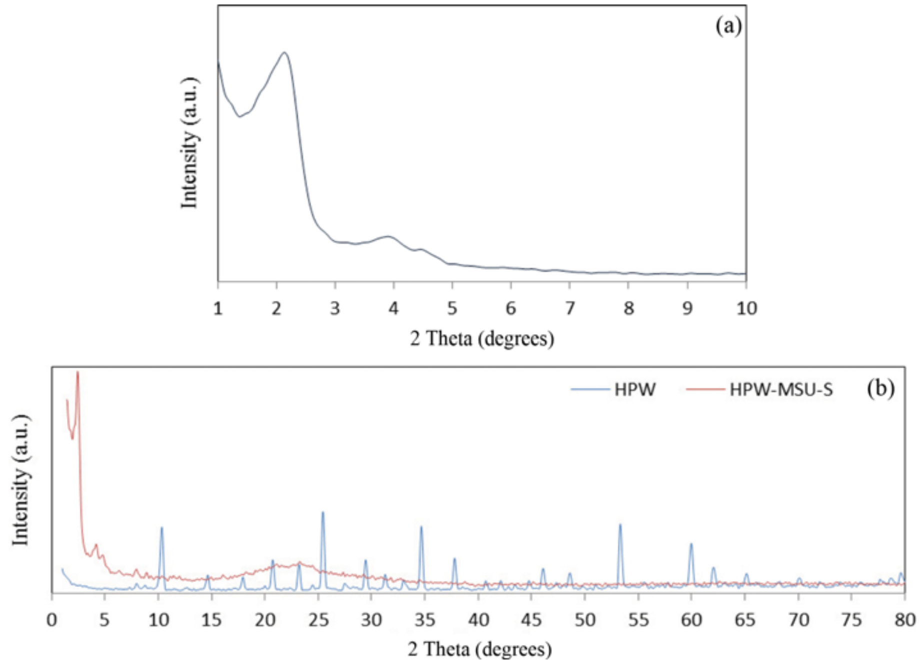

Fig. 1. (a) Low angle XRD pattern of MSU-S catalyst. (b) High-angle XRD patterns of pure HPW and MSU-S material modified with 10% wt HPW with direct synthesis.

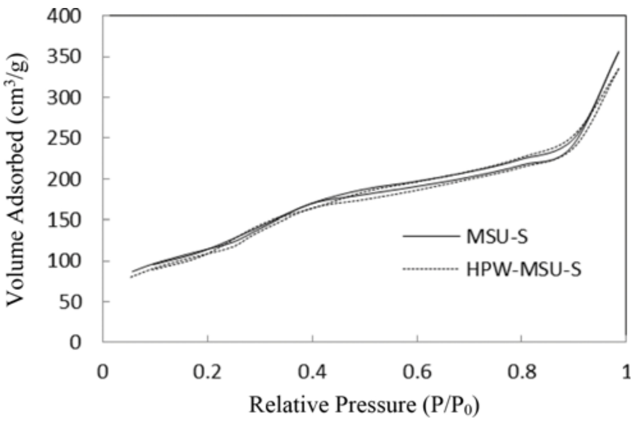

Fig. 2. N_2 adsorption-desorption isotherms for MSU-S and HPW-MSU-S catalysts.

Table 1. Acidity content and textural properties of MSU-S and HPW-MSU-S catalysts

Catalyst	S_{BET} [m^2g^{-1}]	D_{pore} [Å]	V_{pore} [cm^3g^{-1}]	T_d [°C]	S_{ta} [mmol NH_3g^{-1}]
MSU-S	680	24.3	0.65	206	0.271
HPW-MSU-S	652	23.2	0.58	210	0.386

type IV according to the IUPAC classification. The pronounced capillary condensation located at the relative pressure P/P_0 between 0.2 and 0.4 representing a typical of a material possessing a uniform and narrow pore distribution [15,16].

The BET surface area, average pore diameter and pore volume data for MSU-S and HPW-MSU-S catalysts are tabulated in Table 1. From BET results, there is no significant difference between the specific area of HPW-MSU-S and the parent catalyst showing the perfect dispersion of heteropoly acid molecule in the structure of MSU-S catalyst. There is also a slight difference in average pore diameters and total pore volume of these two catalysts.

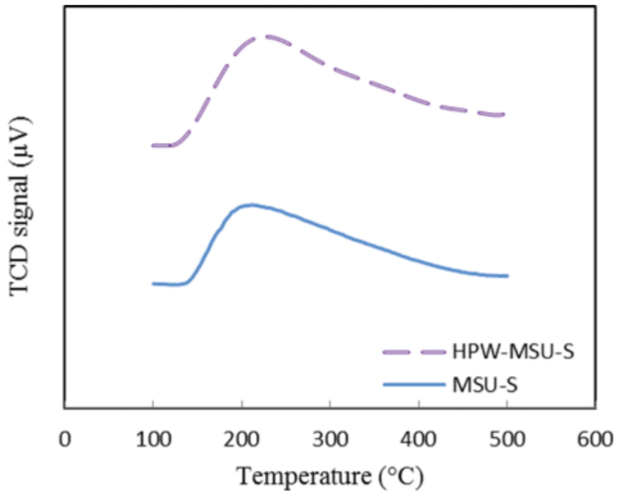

Fig. 3. NH_3-TPD profile of MSU-S and HPW-MSU-S catalysts.

1-3. NH_3-TPD Results

The NH_3-TPD spectra of the MSU-S and HPW-MSU-S powders are shown in Fig. 3. Desorption temperature is an indication of the acid strength of the catalyst; the amount of desorbed ammonia is represented by the acidity amount, which is estimated from the area under each of desorption profiles [17]. From the data in Table 1, it is clear that the amount of acidic sites of the HPW-MSU-S catalyst is more than MSU-S catalyst. It is also verified by the Fig. 3 that the area under the desorption profile of

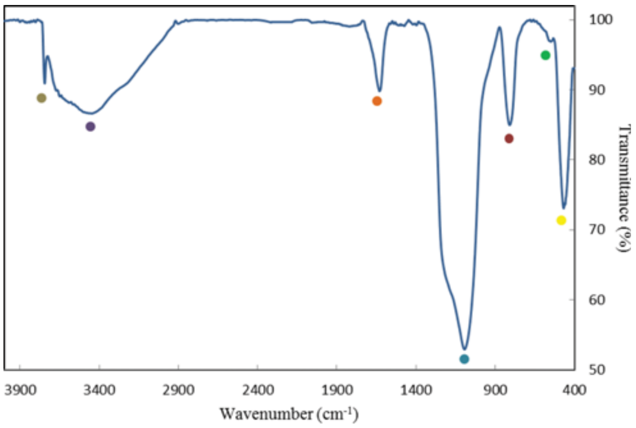

Fig. 4. FT-IR spectra of MSU-S catalyst.

HPW-MSU-S is more than the parent catalyst.

1-4. FT-IR Spectra Results

FT-IR spectra of the MSU-S catalyst are shown in Fig. 4, presenting a band at about 549 cm^{-1} which proves the characteristic of five membered ring subunits, which is an indication of the presence of zeolite (MFI) microdomains [15]. The absorption band observed at approximately 3,447 cm^{-1} is assigned to the stretching vibrations of -OH units in the adsorbed water, and a band at 3,743 cm^{-1} is potentially associated with the asymmetry OH stretching vibrations of silanol groups located at the external surface of the mesoporous materials. The Si-OH deformational vibrations of adsorbed molecules produce the absorption band at approximately 1,630 cm^{-1}. The absorption band at 1,094 cm^{-1} and a band at 809 cm^{-1} are assigned to internal and external asymmetric Si-O stretching modes. The band at 468 cm^{-1} is attributed to tetrahedral Si-O bending modes [18].

FT-IR spectra of HPW-MSU-S catalyst were also conducted (not shown), but no specific band of keggin structure was observed. Range of keggin structure band in FT-IR spectra is between 800-1,000 cm^{-1} [19], but displacement can occur due to perturbation of the keggin structure, which is because of interaction between silica and keggin unit of HPW. It is believed that perturbation is strong in direct synthesis; therefore, overlapping is highly probable.

2. Catalytic Tests

Methanol conversion versus temperature over MSU-S catalyst at WHSVs of 1, 5 and 25 is illustrated in Fig. 5(a) and methanol conversion of MSU-S and HPW-MSU-S catalysts versus temperature at WHSV of 5 h^{-1} is shown in Fig. 5(b). Accordingly, it can be concluded that when temperature increases, methanol conversion rises at each of WHSVs, and the higher WHSVs lead to lower conversions. At WHSV of 25 h^{-1} the space velocity of flowing feed over MSU-S catalyst is high and residence time is low; therefore,

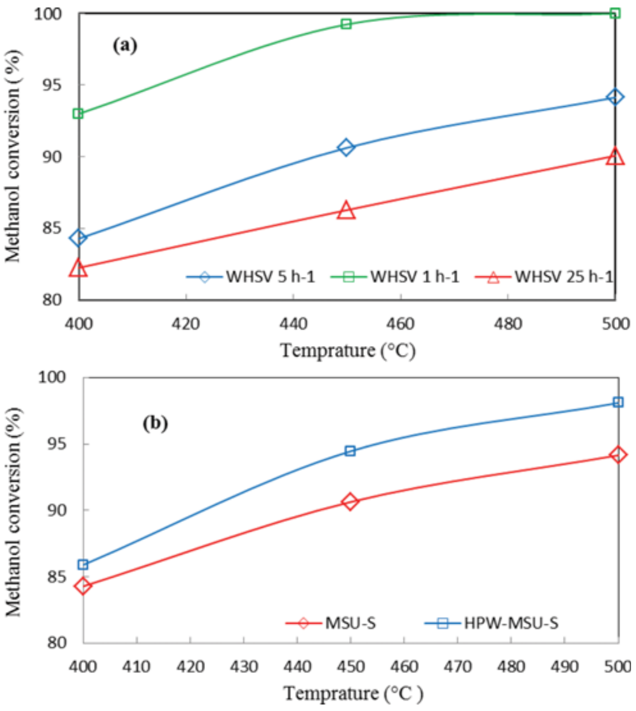

Fig. 5. (a) Methanol conversion over MSU-S catalyst at WHSVs of 1, 5, 25; Temperature range, 400-500 °C; pressure, 2 bar; catalyst loading, 1.5 g. (b) Methanol conversion at WHSV=5 h^{-1} over MSU-S and HPW-MSU-S catalysts. Temperature range, 400-500 °C; pressure, 2 bar; catalyst loading, 1.5 g. Data reported at 30 min of time on stream.

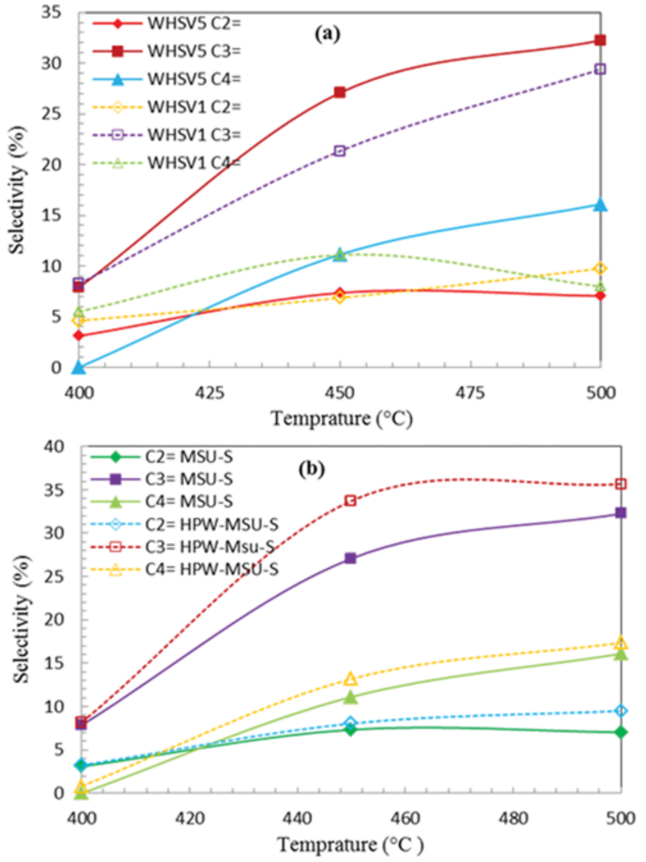

Fig. 6. (a) Selectivity of MSU-S catalyst at WHSV, 1 and 5 h^{-1}; temperature range, 400-500 °C; pressure, 2 bar; catalyst loading, 1.5 g. (b) Selectivity of MSU-S and HPW-MSU-S to olefins at WHSV=5 h^{-1}. Temperature range, 400-500 °C; pressure, 2 bar; catalyst loading, 1.5 g. Data reported at 30 min of time on stream.

Table 2. Selectivity percent of all the products of tested catalysts at 500 (°C), data reported at 30 min of time on stream and pressure of 2 bar

Component	HPW-MSU-S	MSU-S		
	WHSV=5	WHSV=1	WHSV=5	WHSV=25
C1	1.0	12.9	1.4	0.2
$C2^=$	8.2	10.2	7.0	1.3
C2	0.24	2.8	0	0
$C3^=$	35.3	28.8	32.3	4.2
C3	1.19	0	2.8	0
$C4^=$	17.0	8	16.1	0
C4	14.56	12.1	12.9	0
C5+	20.9	8.4	23.6	0
DME	1.59	16.7	3.8	94.3

there is not enough time for methanol to be converted to olefins and higher carbon products and DME is the main product of the reaction, which is considered as an intermediate for production of olefins and other hydrocarbons. Therefore, WHSV of 25 h^{-1} was not considered as a suitable flow rate for methanol conversion to olefins. On the contrary, at WHSV of 1 h^{-1}, the time needed to convert the feed to desired products suffices; the conversion approaches 100%, especially at higher temperatures. Because of high residence time at WHSV of 1 h^{-1}, cracking increases and production of lighter hydrocarbons such as methane and ethylene, specifically methane, rises.

On the other hand, based on Fig. 6(a) and Table 2, MSU-S catalyst showed higher selectivity toward light olefins at WHSV of 5 h^{-1} than WHSV of 1 h^{-1}. Accordingly, because of high tendency to methane production and lower selectivity to light olefins at WHSV of 1 h^{-1}, the optimum weight hourly space velocity was chosen to be 5 h^{-1}. Although conversion is lower at WHSV of 5 h^{-1}, it has higher selectivity toward desired products (Fig. 6(a)); deficiency of lower conversion can be dissolved by recycling unreacted methanol. Therefore, HPW-MSU-S was investigated at WHSV of 5 h^{-1}; HPW-MSU-S catalyst showed higher methanol conversion in comparison with MSU-S catalyst (Fig. 5(b)). This behavior is verified by TPD results which showed HPW-MSU-S catalyst possesses higher amount of acidity than MSU-S catalyst. It also showed higher selectivity to light olefins compared to the parent catalyst at WHSV of 5 h^{-1} (Fig. 6(b)).

Based on the amount of various light olefins produced, the following sequence dominates: $C_3^= > C_4^= > C_2^=$. Higher conversion and selectivity to desired products of HPW-MSU-S catalyst with respect to MSU-S causes the sum of light olefins yield to be higher than the MSU-S catalyst (Fig. 7). Numerical values of light olefins yield at 450 °C and 500 °C are 51.9 and 59.3, respectively, which are greater than those values of MSU-S catalyst (41.2 and 52.1). By comparing the yields of the products of MSU-S catalyst at investigated WHSVs (Fig. 7), it is found that despite the lower methanol conversion at WHSV of 5 h^{-1} over MSU-S catalyst than WHSV of 1 h^{-1}, the sum of light olefins yield is higher at 450 and 500 °C. At WHSV of 25 h^{-1}, not significant amount of light olefins was produced; the conversion is at the lowest value among two other WHSVs and the product is mainly comprised of DME. Comparing yields of the products of two catalysts (MSU-S and HPW-MSU-S) at WHSV of 5 h^{-1} and varying temperatures, the HPW-MSU-S catalyst yield of light olefins is higher and possesses the highest amount of light olefins production, approximately around 60% at WHSV of 5 h^{-1} and 500 °C.

Table 3. The ratio of propylene to ethylene production, data reported at 30 min of time on stream and pressure of 2 bar

Temperature (°C)	$C3^=/C2^=$			
	MSU-S WHSV 1	MSU-S WHSV 5	MSU-S WHSV 25	HPW-MSU-S WHSV 5
400	1.78	2.54	1	2.52
450	3.11	3.68	2.33	4.1
500	2.82	4.57	3.14	4.30

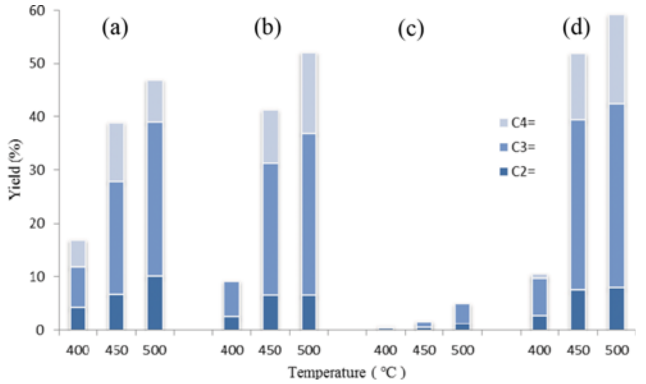

Fig. 7. Yield of (a) MSU-S at WHSV=1 h^{-1} (b) MSU-S at WHSV=5 h^{-1} (c) MSU-S at WHSV=25 h^{-1} (d) HPW-MSU-S at WHSV=5 h^{-1}. Temperature range, 400-500 °C; pressure, 2 bar; catalyst loading, 1.5 g.

Based on the data presented in Tab. 3, there is an increase in the $C_3^=/C_2^=$ ratio for MSU-S catalyst at WHSV of 5 and 25 h^{-1} as temperature rises. But at WHSV of 1 h^{-1}, it is observed that in transition between temperatures of 450 and 500 °C, propylene to ethylene ratio has fallen. As described beforehand, at WHSV of 1 h^{-1}, due to higher residence time, there is enough time for the products to crack and be converted to lighter hydrocarbons such as methane and ethylene. HPW-MSU-S catalyst also follows the same behavior as MSU-S catalyst; the propylene to ethylene ratio rises while increasing temperature. This higher propylene yield compared to ethylene can be attributed to the larger pore diameters of MSU-S (24.3 Å) and HPW-MSUS-S (23.2 Å). On the contrary, tests conducted on the other zeolites possessing smaller diameters (ZSM-5 (5.4 Å), SAPO-34 (3.8 Å)) [8] showed higher tendency to produce ethylene. The propylene-to-ethylene ratio varies between 1 to 2.5 for ZSM-5 and 0.14 to 1.66 and 2.1 for SAPO-34 in temperature range of 250 °C to 500 °C [3,4,20,21].

As mentioned in the introduction, higher ratio of propylene to ethylene production is required for market demand; therefore, MSU-S and HPW-MSU-S catalysts can be considered as novel catalysts for high ratio of propylene-to-ethylene production.

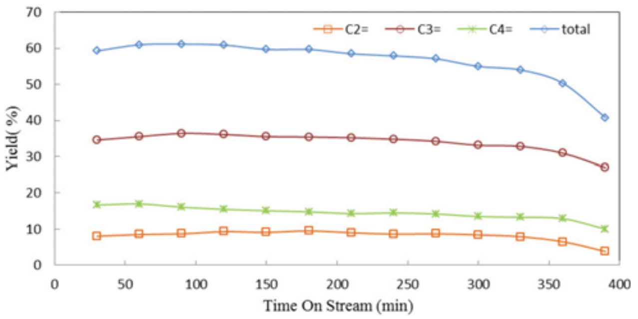

Fig. 8. Life time of HPW-MSU-S catalyst at 500 °C and WHSV of 5 h^{-1}.

Stability of the HPW-MSU-S catalyst at WHSV of 5 h^{-1} and temperature of 500 °C was evaluated and the result is shown in Fig. 8. As observed, due to the enhanced hydrothermal stability of MSU-S, the catalyst showed significant stability, which can be attributed either to the nature of MSU-S catalyst or the synthesis method applied for incorporation of HPW.

CONCLUSION

MSU-S catalyst was synthesized and promoted by HPW via a direct synthesis to reach high dispersion of HPW in the parent catalyst. For the first time, MSU-S and HPW-MSU-S catalysts were employed for the selective production of light olefins from methanol. The sum of light olefins yield over MSU-S and HPW-MSU-S at 500 °C and WHSV of 5 h^{-1} reached to 52 and nearly 60% with exceptional propylene to ethylene ratio of 4.57 and 4.3, respectively. Hence; MSU-S and HPW-MSU-S catalysts can be considered as novel catalysts for high propylene to ethylene ratio production.

NOMENCLATURE

Symbols

$C3^=$: ethylene
$C3^=$: propylene
$C4^=$: butylene
D_{pore} : average pore diameter
S_{BET} : specific surface area
S_{ta} : total acid sites
T_d : maximum desorption temperature
V_{pore} : total pore volume

Abbreviations

BET : Brunauer-Emmett-Teller
DME : dimethyl ether
FID : flame ionization detector
FTIR : fourier transform infrared spectroscopy
MSU : michigan state university
MTG : methanol to gasoline
MTO : methanol to olefin
NH_3-TPD : temperature-programmed desorption of ammonia
SAPO : silica alumina phosphate
TCD : thermal conductivity detector
WHSV : weight hourly space velocity
XRD : X-ray diffraction

REFERENCES

1. M. Stöcker, *J. Micropor. Mesopor. Mater.*, **29**, 3 (1999).
2. M. Salmasi, S. Fatemi and S. J. Hashemi, *J. Scientia Iranica.*, **19**, 1632 (2012).
3. L. Travalloni, A. C. L. Gomes, A. B. Gaspar and M. a. P. da Silva, *J. Catal. Today*, **133**, 406 (2008).
4. J. Q. Chen, A. Bozzano, B. Glover, T. Fuglerud and S. Kvisle, *J. Catal. Today*, **106**, 103 (2005).
5. S. Soundararajan, A. K. Dalai and F. Berruti, *J. Fuel*, **80**, 1187 (2001).
6. H. Sh. Pajaie and M. Taghizadeh, *Chem. Eng. Technol.*, **38**, 931 (2015).
7. H. G. Kim, K. Y. Lee, H. G. Jang, Y. S. Song and G. Seo, *Korean J. Chem. Eng.*, **27**(6), 1773 (2010).
8. X. Meng, H. Huang, Q. Zhang, C. Li and Q. Cui, *Korean J. Chem. Eng.*, **33**(4), 1239 (2016).
9. A. Taheri Najafabadi, S. Fatemi, M. Sohrabi and M. Salmasi, *J. Ind. Eng. Chem.*, **18**, 29 (2012).
10. N. Fatourehchi, M. Sohrabi, S. J. Royaee and S. M. Mirarefin, *J. Chem. Eng. Res. Des.*, **89**, 811 (2011).
11. M. Kaarsholm, B. Rafii, F. Joensen, R. Cenni, J. Chaouki and G. S. Patience, *J. Ind. Eng. Chem. Res.*, **49**, 29 (2010).
12. J. Wang, W. Hua, Y. Yue and Z. Gao, *J. Bio. Tech.*, **101**, 7224 (2010).
13. S. Rashidi, M. R. Khosravi Nikou and B. Anvaripour, *Micropor. Mesopor. Mater.*, **211**, 134 (2015).
14. Z. Zhang, Y. Han, F. Xiao and S. Qiu, *J. Am. Chem. Soc.*, **123**(21), 5014 (2001).
15. K. S. Triantafyllidis, E. F. Iliopoulou, E. V. Antonakou, A. a. Lappas, H. Wang and T. J. Pinnavaia, *Micropor. Mesopor. Mater.*, **99**, 132 (2007).
16. B. C. Gagea, Y. Lorgouilloux, Y. Altintas, P. a. Jacobs and J. a. Martens, *J. Catal.*, **265**, 99 (2009).
17. J. P. Lourenço, A. Fernandes, C. Henriques and M. F. Ribeiro, *Micropor. Mesopor. Mater.*, **94**, 56 (2006).
18. M. Adjdir, T. Ali-Dahmane, F. Friedrich, T. Scherer and P. G. Weidler, *J. Appl. Clay Sci.*, **46**, 185 (2009).
19. G. R. Moradi, F. Yaripour and P. Vale-Sheyda, *J. Fuel. Proc. Technol.*, **91**, 461 (2010).
20. C. Huo, J. Ouyang and H. Yang, *J. Sci. Rep.*, **4**, 3682 (2014).
21. A. Llanos, L. Melo, F. Avendano, A. Montes and J. L. Brito, *J. Catal. Today*, **133**, 20 (2008).
22. M. Salmasi, S. Fatemi and A. Taheri Najafabadi, *J. Ind. Eng.*, **17**, 755 (2011).
23. D. Chen, K. Moljord, T. Fuglerud and A. Holmen, *J. Micropor. Mesopor. Mater.*, **29**, 191 (1999).
24. Y. Liu, W. Zhang and T. Pinnavaia, *J. Chem. Int. Ed.*, **113**, 1295 (2001).